pH-dependent catalytic activity of Au and Pd-based hybrid cryogels by investigating the acid/base nature of the polymeric phase

Stefano Scurti[1], Giuseppe Proietto Salanitri[1,3], Tommaso Mecca[4], Elena Rodríguez-Aguado[5], Juan Antonio Cecilia[5], Giusy Curcuruto[3], Sabrina Carola Carroccio[3], Daniele Caretti[1], Nikolaos Dimitratos[1,2*]

[1] Industrial Chemistry "Toso Montanari" Department, University of Bologna, Viale Risorgimento 4, 40136 Bologna, Italy

[2] Center for Chemical Catalysis-C3, Alma Mater Studiorum Università di Bologna, Viale Risorgimento 4, 40136 Bologna, Italy

[3] Institute for Polymers, Composites and Biomaterials (IPCB) – CNR, Via Paolo Gaifami 18, 95126 Catania, Italy

[4] Institute for Biomolecular Chemistry (ICB) – CNR , Via Paolo Gaifami 18, 95126 Catania, Italy

[5] Departamento de Química Inorgánica, Cristalografía y Mineralogía (Unidad Asociada al ICP-CSIC), Facultad de Ciencias, Universidad de Málaga, Campus de Teatinos, 29071 Málaga, Spain

*nikolaos.dimitratos@unibo.it; Industrial Chemistry "Toso Montanari" Department, University of Bologna, Viale Risorgimento 4, 40136 Bologna, Italy

Cryogels characterization

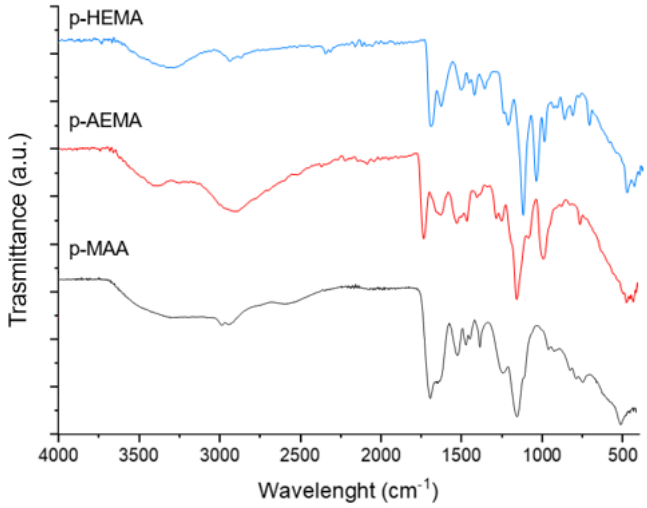

Fig. S1. ATR-IR spectra of synthesized polymeric cryogels.

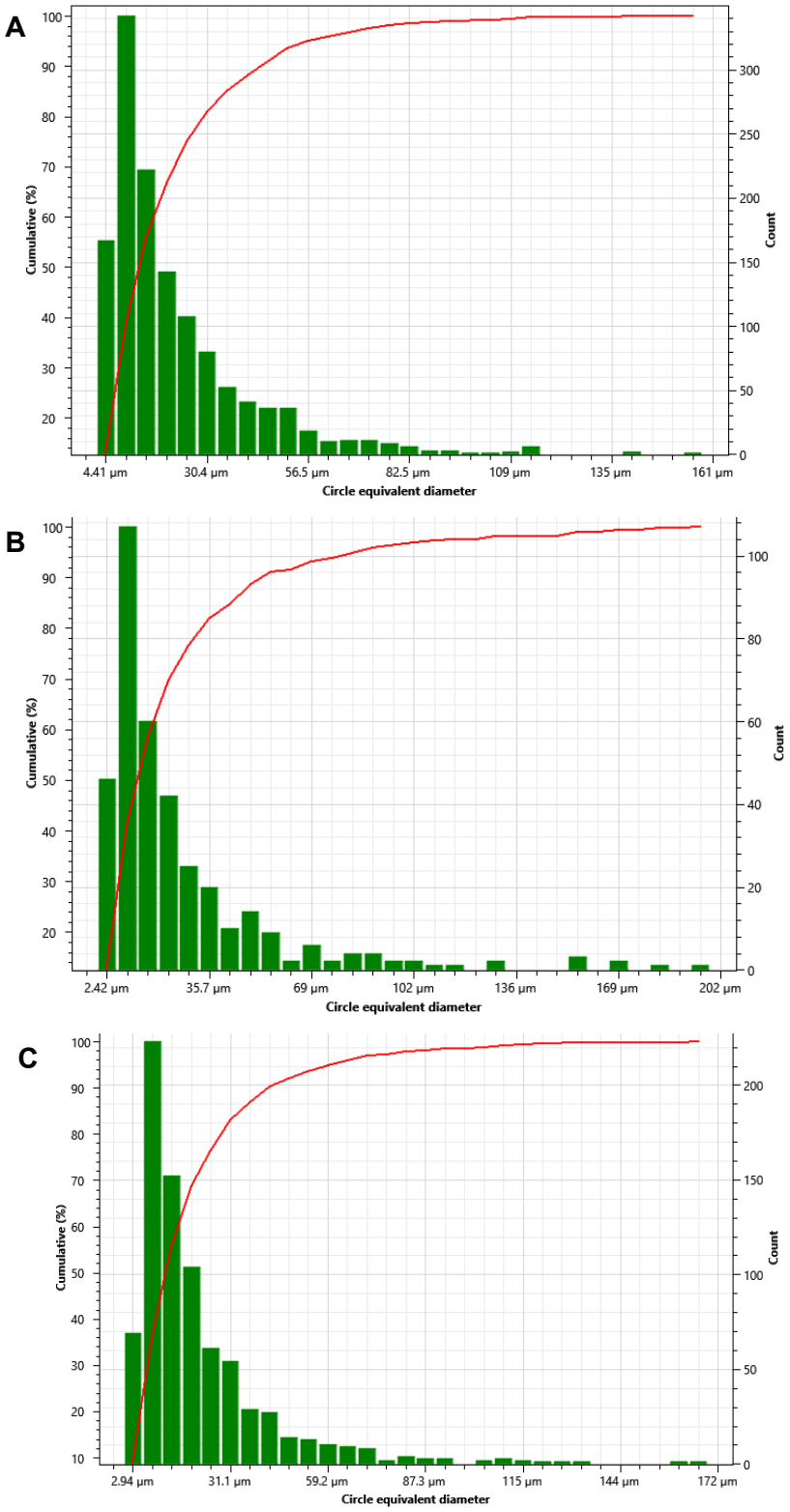

Fig. S2. Circular equivalent diameter distribution for the bare cryogels: p-HEMA (A), p-MAA (B) and p-AEMA (C).

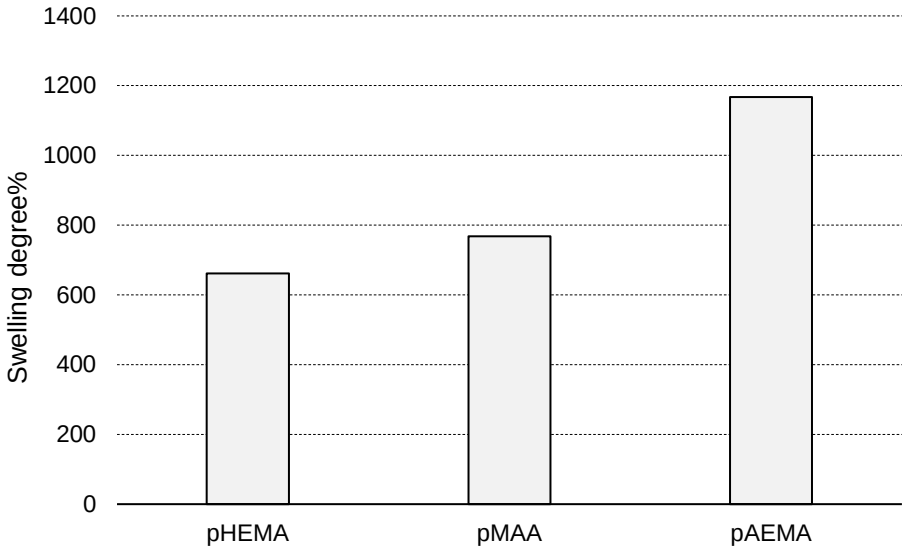

Fig. S3. Swelling degree % for the bare cryogels.

Table S1. Swelling test data.

Sample	m_w (g)	m_d (g)	SD%
p-HEMA	1.36	0.18	660
p-MAA	0.61	0.07	770
p-AEMA	1.52	0.12	1170

Characterization of hybrid metal-polymer nanocatalysts

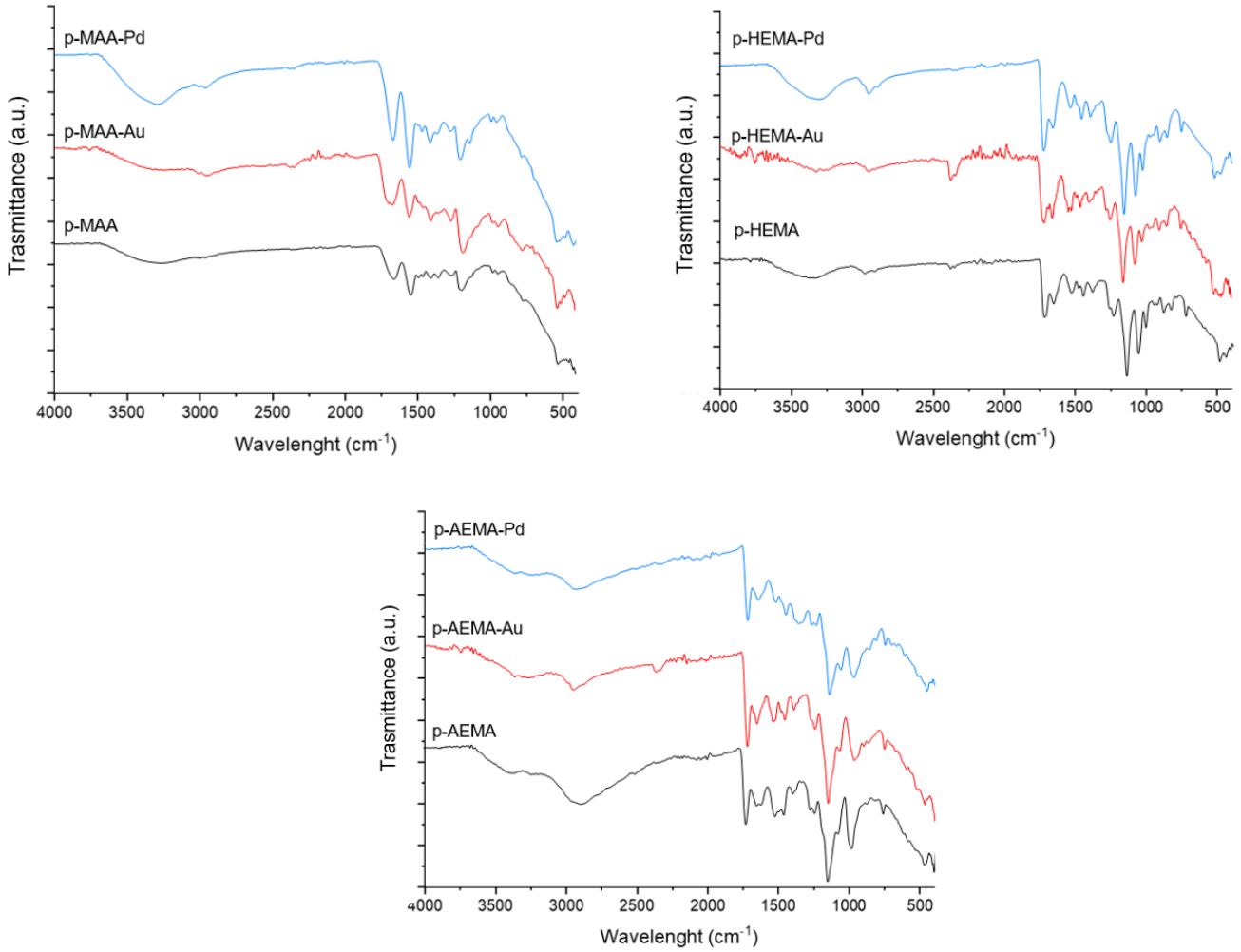

Fig. S4. Comparison between ATR-IR spectra of bare and functionalized cryogels with Au e Pd nanoparticles for each sample prepared.

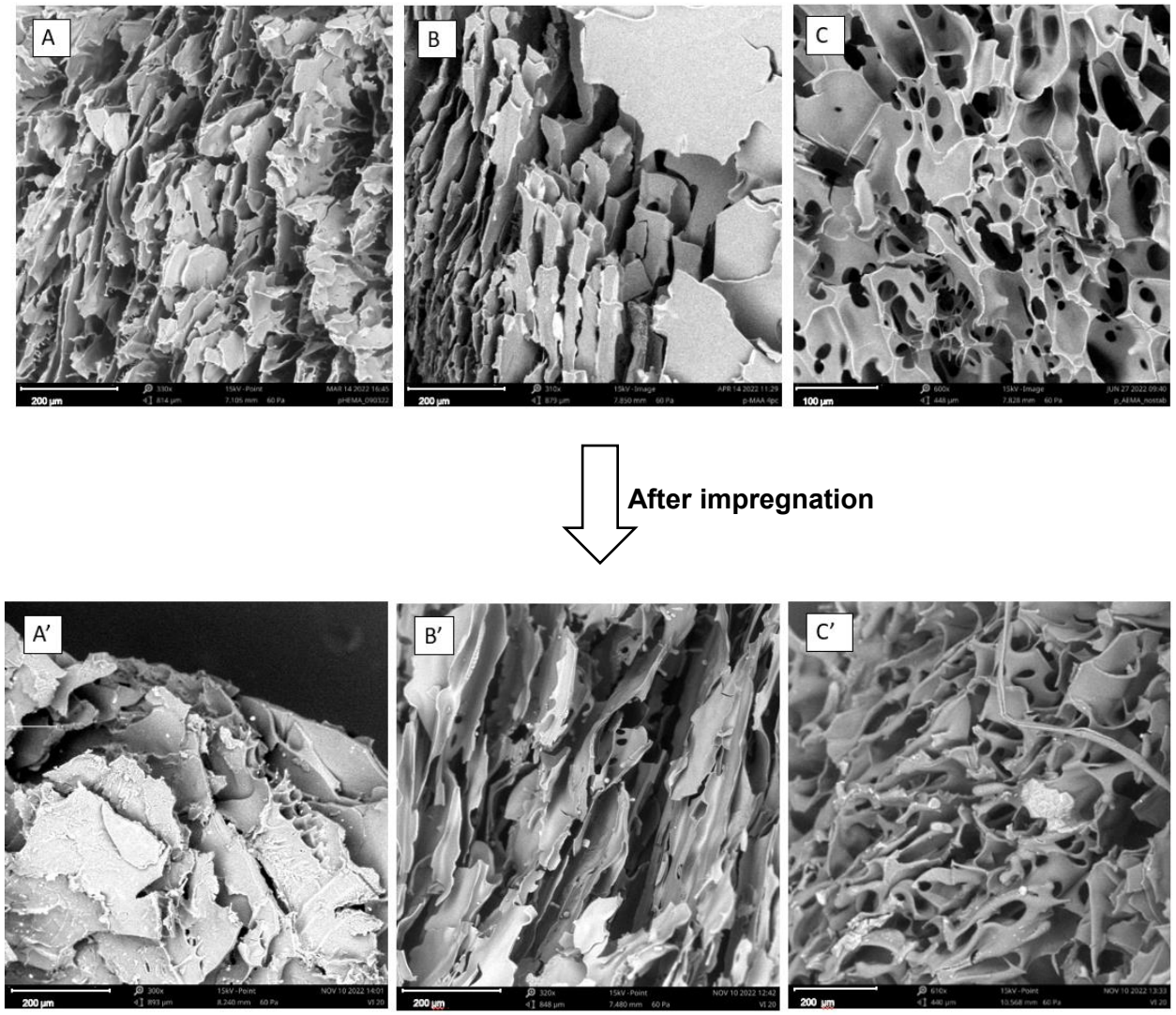

Fig. S5. SEM images before and after the impregnation phase (the images reported are related to the Au-based catalysts: (A-A') p-HEMA, (B-B') p-MAA, (C-C') p-AEMA.

Catalytic tests

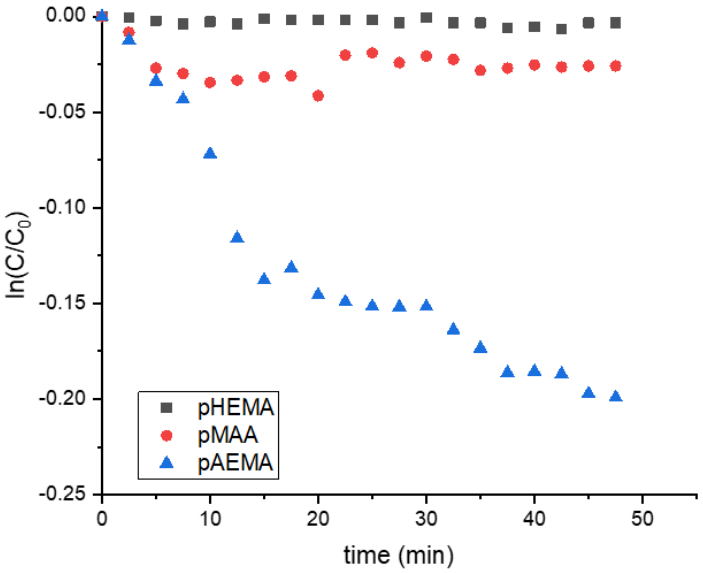

Fig. S6. Adsorption test for the bare cryogels: 25 mL of 4–NP ($2 \cdot 10^{-4}$ M), 25 mL of $NaBH_4$ ($9.0 \cdot 10^{-3}$ M) at 25 °C and 500 rpm.

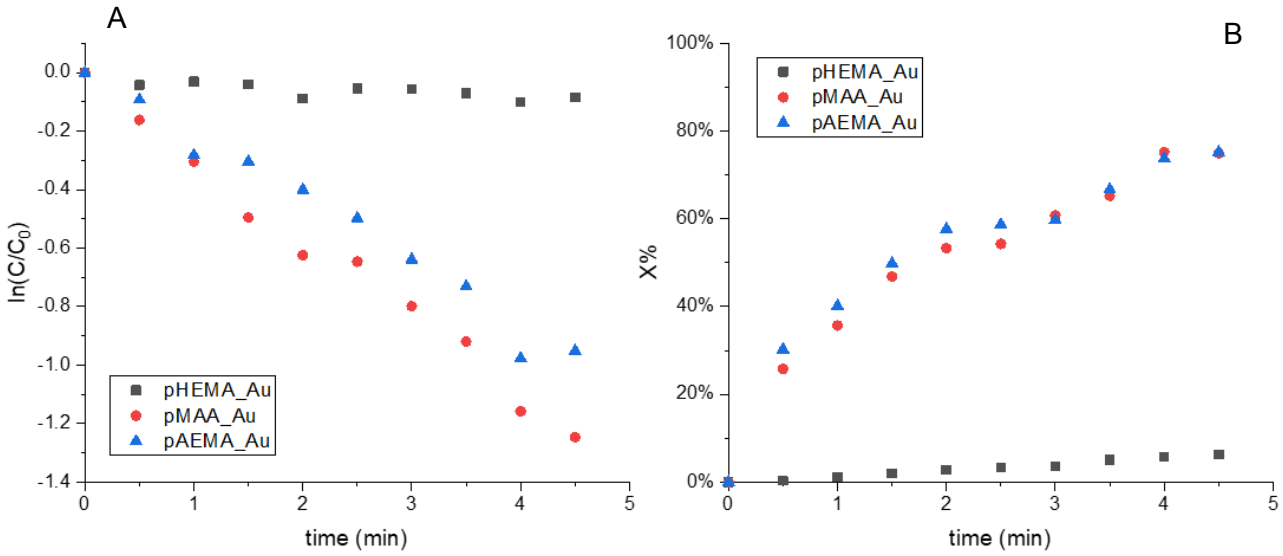

Fig. S7. Pseudo–first−order kinetic plot (A) and (B) conversion plot for Au-based hybrid catalysts. The reduction of 4–NP was carried out using 25 mL of 4–NP ($2 \cdot 10^{-4}$ M), 25 mL of $NaBH_4$ ($9.0 \cdot 10^{-3}$ M), 4 mg of catalyst at 25 °C and 500 rpm.

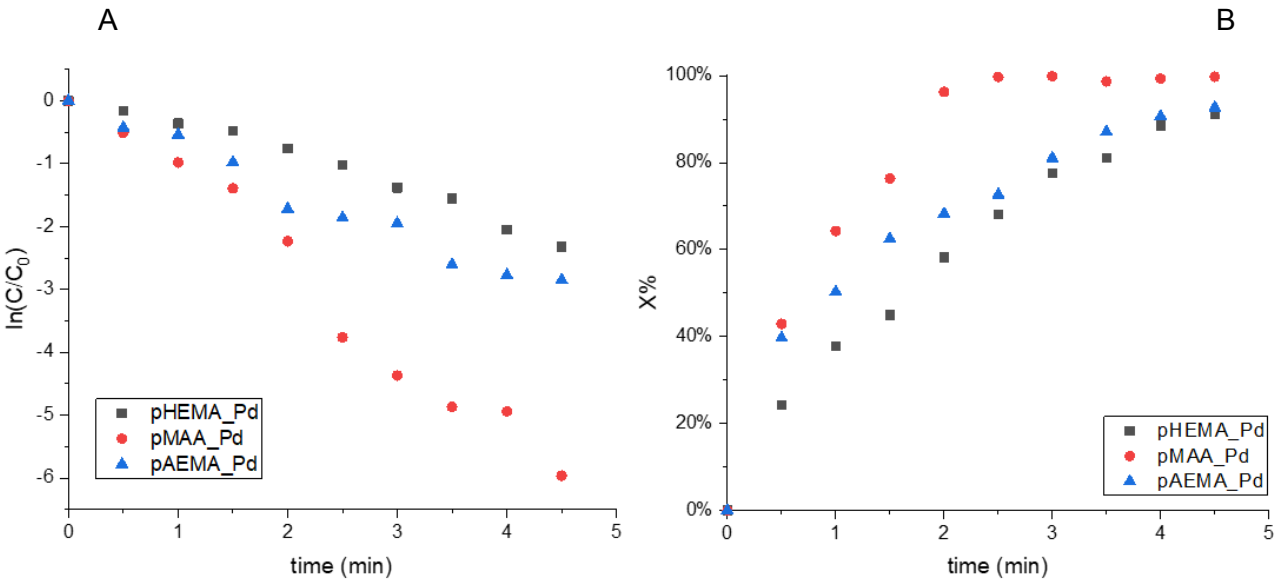

Fig. S8. Pseudo–first–order kinetic plot (A) and (B) conversion plot for Pd-based hybrid catalysts. The reduction of 4–NP was carried out using 25 mL of 4–NP ($2 \cdot 10^{-4}$ M), 25 mL of $NaBH_4$ ($9.0 \cdot 10^{-3}$ M), 4 mg of catalyst at 25 °C and 500 rpm.

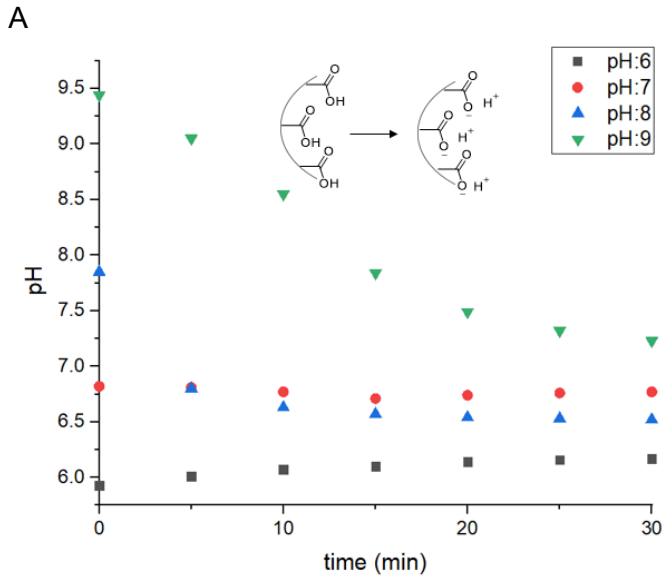

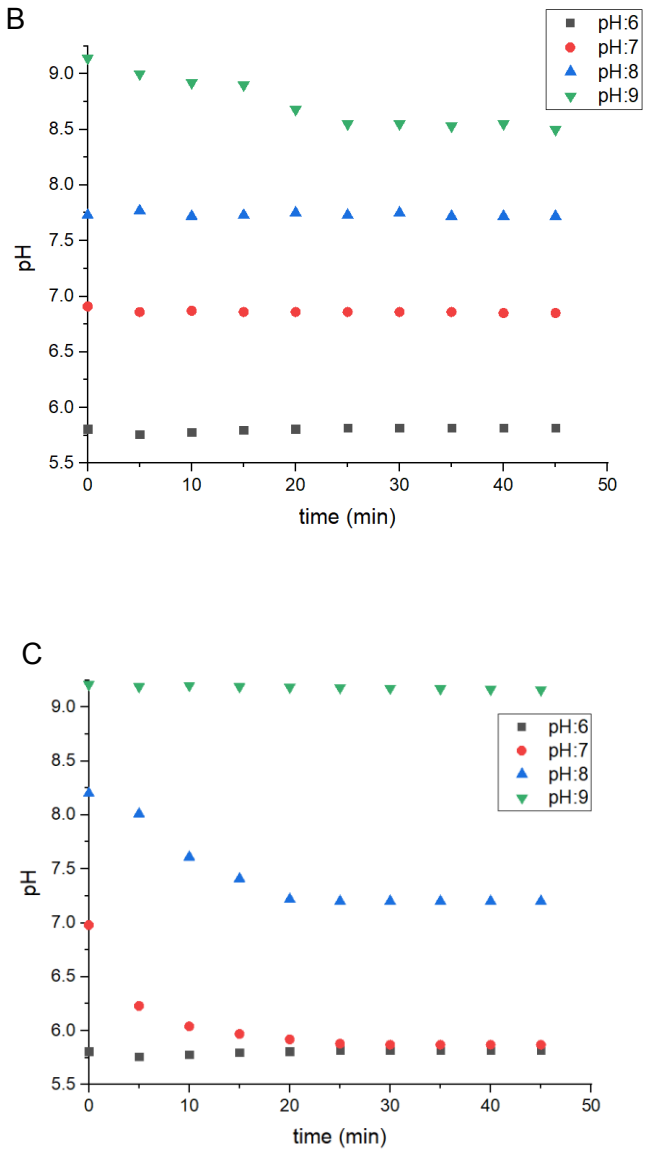

Fig. S9. pH measures as a function of time starting from values in the range of the reaction pH for bare cryogels: p-MAA (A), p-HEMA (B) and p-AEMA (C).

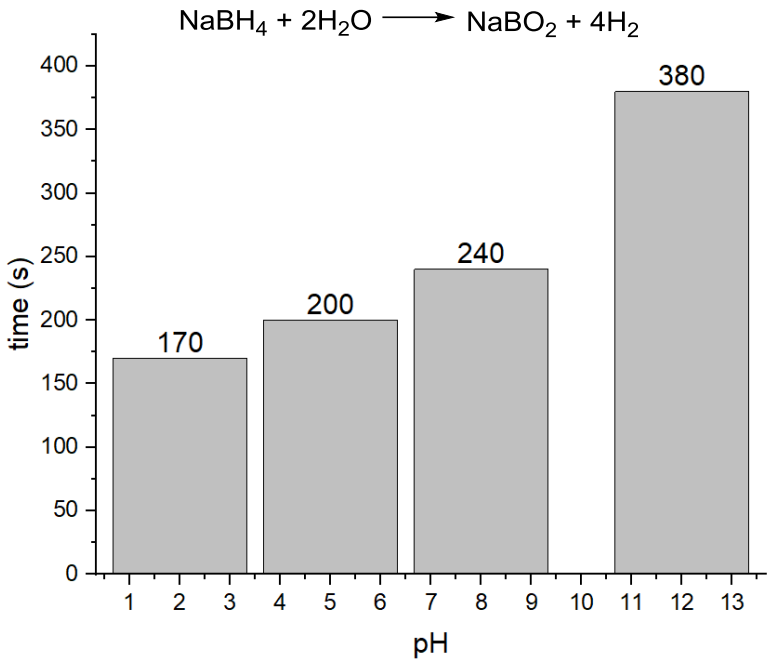

Fig. S10. Evaluation of $NaBH_4$ decomposition time as a function of pH.

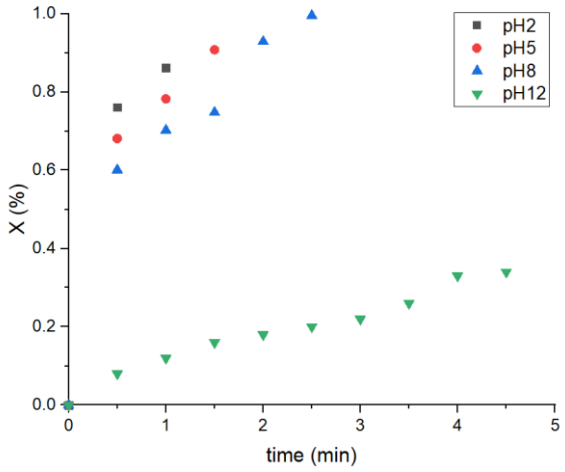

Fig. S11. Conversion plot related to p-MAA_Pd for the 4–NP reduction carried out using 25 mL of 4–NP ($2 \cdot 10^{-4}$ M), 25 mL of $NaBH_4$ ($9.0 \cdot 10^{-3}$ M), 4 mg of catalyst at different pH.